NeuroImage 118 (2015) 237–247

Contents lists available at ScienceDirect

NeuroImage

journal homepage: www.elsevier.com/locate/ynimg

Developmental changes in spontaneous electrocortical activity and network organization from early to late childhood☆

Vladimir Miskovic [a,b,*], Xinpei Ma [c], Chun-An Chou [a,c], Miaolin Fan [c], Max Owens [a,b], Hiroki Sayama [a,c], Brandon E. Gibb [a,b]

[a] Center for Affective Science, State University of New York at Binghamton, USA
[b] Department of Psychology, State University of New York at Binghamton, USA
[c] Department of Systems Science and Industrial Engineering, State University of New York at Binghamton, USA

ARTICLE INFO

Article history:
Received 26 February 2015
Accepted 3 June 2015
Available online 7 June 2015

ABSTRACT

We investigated the development of spontaneous (resting state) cerebral electric fields and their network organization from early to late childhood in a large community sample of children. Critically, we examined electrocortical maturation across one-year windows rather than creating aggregate averages that can miss subtle maturational trends. We implemented several novel methodological approaches including a more fine grained examination of spectral features across multiple electrodes, the use of phase-lagged functional connectivity to control for the confounding effects of volume conduction and applying topological network analyses to weighted cortical adjacency matrices. Overall, there were major decreases in absolute EEG spectral density (particularly in the slow wave range) across cortical lobes as a function of age. Moreover, the peak of the alpha frequency increased with chronological age and there was a redistribution of relative spectral density toward the higher frequency ranges, consistent with much of the previous literature. There were age differences in long range functional brain connectivity, particularly in the alpha frequency band, culminating in the most dense and spatially variable networks in the oldest children. We discovered age-related reductions in characteristic path lengths, modularity and homogeneity of alpha-band cortical networks from early to late childhood. In summary, there is evidence of large scale reorganization in endogenous brain electric fields from early to late childhood, suggesting reduced signal amplitudes in the presence of more functionally integrated and band limited coordination of neuronal activity across the cerebral cortex.

© 2015 Elsevier Inc. All rights reserved.

Spontaneous, ongoing fluctuations of large-scale neuronal activity are often the most directly visible features of electroencephalographic (EEG) and magnetoencephalographic (MEG) recordings of brain function. Traditionally viewed as reflecting only non-deterministic signal stochasticity, there is now increasing evidence that brains are autonomously active systems and that endogenous fluctuations exhibit a coherent functional architecture that interacts with subsequent stimulus processing (Deco et al., 2013; Northoff et al., 2010; Raichle, 2010). The intrinsic activity of neuronal populations accounts for much of the variability in stimulus- and task-evoked responses (Arieli et al., 1996; Fontanini and Katz, 2008; Kenet et al., 2003; MacLean et al., 2005; Ringach, 2009) including the variability in neurovascular reactivity that is quantified by functional magnetic resonance imaging (fMRI) methods (Becker et al., 2011). Recent computational modeling evidence suggests that it is possible to mathematically represent large populations of cortical neurons as self-organizing coherent units that are governed by a set of dynamical equations with a rich spatiotemporal repertoire (Betzel et al., 2012; Hipp et al., 2012; Liu et al., 2010) in the absence of external perturbations (Deco et al., 2011, 2013). The diverse and continuously changing ensemble of states that is explored by cortical circuits in the absence of stimulus input is shaped both by the intrinsic oscillatory properties of neurons as well as by the spatial spreading of synchronization due to recurrent connectivity (Hipp et al., 2012; Sporns, 2011). Brain development is associated with a general increase in the diversity of spontaneous cortical states, a fact that may underlie increases in sophistication of information processing into adolescence and early adulthood (Vakorin et al., 2011, 2013; Koening et al., 2002; Lippé et al., 2009; McIntosh et al., 2008). Accordingly, charting the maturational profiles of spontaneous neuroelectrical activity and the

☆ This project was supported by National Institute of Mental Health grant MH098060 awarded to B. E. Gibb and a Binghamton University (SUNY) Interdisciplinary Collaborative Grant awarded to V. Miskovic. We would like to thank Devra Alper, Cope Feurer, Eric Funk, Effua Sosoo, Katie Burkhouse, Mary Woody, Anastacia Kudinova, Aliona Tsypes and Thomas Nguyen for their help in conducting assessments for this project.

* Corresponding author at: Department of Psychology, State University of New York at Binghamton, Binghamton, NY 13902-6000, USA.
E-mail address: miskovic@binghamton.edu (V. Miskovic).

http://dx.doi.org/10.1016/j.neuroimage.2015.06.013
1053-8119/© 2015 Elsevier Inc. All rights reserved.

development of large-scale cortical oscillatory networks has emerged as an active area of research inquiry (Palva and Palva, 2012; Uhlhaas et al., 2010), one that can reveal the neural infrastructure that underlies both healthy and disordered perceptual, cognitive and affective capacities.

To date, a substantial amount of evidence exists pertaining to age-dependent changes in spontaneous and event-related electrophysiological activity. In terms of spontaneous spectral EEG/MEG power, a general trend is for a decrease across all frequency bands, particularly in the amount of slow wave (delta and theta band) rhythmic activity (see Segalowitz et al., 2010; Uhlhaas et al., 2010 for substantive reviews). Simultaneously, there is a relative redistribution of power in the higher frequency bands (such as alpha and beta) along with a shift in the peak frequency of the dominant alpha-band with increased brain maturation (Chiang et al., 2011; Cragg et al., 2011; Dustman et al., 1999; Somsen et al., 1997). Although the precise neurophysiological mechanisms that underlie these age-dependent changes in electrocortical activity are difficult to identify using *in vivo* recordings in healthy humans, convergent evidence using techniques with superior spatial resolution can furnish plausible hypotheses (Paus, 2007; Uhlhaas et al., 2010). In a unique study that recorded spontaneous EEG activity and structural MRI scans from the same subjects, ranging in age from 10 to 30 years of age, Whitford et al. (2007) observed parallel curvilinear age-related declines in the amount of slow wave EEG power and cortical gray matter density. The authors attributed the maturational decrease in slow wave EEG activity to a neurophysiological mechanism involving neuropil reduction, primarily owing to synaptic pruning (see also Buchmann et al., 2011). A putative causal link between gray matter density and EEG power is inherently plausible, since the latter emerges as the population-level result of highly synchronous post-synaptic potentials of cortical pyramidal neurons with tangential and radial dipolar moments (Nunez and Srinivasan, 2006).

The diverse repertoire of spontaneous cortical activity emerges not only as a result of the intrinsic oscillatory activity of neurons and neuronal populations, but also as a result of dynamically changing "cortical clouds of connectivity" (Horton and Adams, 2005) that establish transient networks or assemblies of widespread neuronal populations (Varela et al., 2001). Currently, there are two known neuronal intrinsic coupling modes—one is mediated by phase synchronization of band-limited brain signals and the other by the aperiodic fluctuations of amplitude envelopes (Engel et al., 2013). White matter pathways provide a structural basis for the sculpting of dynamic functional connectivity in the brain (Sporns et al., 2000), although there is only partial overlap between structural and functional brain connectivity (Damoiseaux and Greicius, 2009). Complementing age-related thinning of cortical gray matter, there is a very linear increase of white matter density across age, related to the maturation of long-distance fascicular pathways (Casey et al., 2005; Giedd et al., 1999; Gogtay et al., 2004; Paus et al., 2008). Increases in myelination and white matter density have been suggested to underlie shifts in the peak frequency of the posterior alpha-band rhythm that are observed across age (Segalowitz et al., 2010). In addition to these regional changes in alpha-band cycling, maturation of white matter pathways and synaptic tuning is likely to be reflected in the organization of resting state cortical networks—*i.e.*, functionally coupled brain networks that are detectable in the absence of explicit cognitive or affective tasks (Laufs, 2008). Indeed, evidence from fMRI studies suggests that functional connectivity within several resting state brain networks progresses from a more local organization in childhood to an increasingly integrated and spatially distributed architecture in adolescence and young adulthood (Fair et al., 2007, 2009; Supekar et al., 2009). A general finding across these studies is that short range functional connectivity is gradually replaced by more distant, long range functional connections. Using multivariate pattern analyses, Dosenbach et al. (2010) demonstrated that brain maturity could be predicted by the functional segregation of local regions combined with greater integration of distant cortical areas via links running along the anterior–posterior axis. Although functional connectivity *within* particular resting-state networks (e.g., fronto-parietal task control network) seems to strengthen across age (Fair et al., 2007), ontogeny seems to be associated primarily with increased integration *between* networks (Betzel et al., 2014).

Additional evidence for age-related changes in spontaneous functional brain network organization comes from EEG/MEG studies that are uniquely able to characterize phase-dependent modes of intrinsic neuronal coupling (Engel et al., 2013). Preliminary evidence from multi-modal imaging studies suggests that electrophysiological measures of connectivity partially map onto the structural integrity of white matter tracts (Chu et al., 2015; Teipel et al., 2009; Thatcher et al., 1998). In a large study spanning the ranges from 6 months to 7 years of age, Thatcher (1992) reported cyclical increases in short- and long range EEG coherence that were punctuated by non-linear growth spurts. Subsequently these non-linear effects were formalized into a "predator–prey" model of cortico-cortical connections, in which the short and long-range association fibers compete for space in the supragranular layers of cortex, with the suggestion that the former expand and the latter contract in older children (Thatcher et al., 2008). However, contrary to this suggestion, and in agreement with recent fMRI studies (Betzel et al., 2014; Dosenbach et al., 2010; Fair et al., 2007, 2009; Supekar et al., 2009), Barry et al. (2004) reported evidence that long range EEG coherence increases across multiple frequency bands from 8 to 12 years age. Similar age-related increases in functional connectivity have been demonstrated to continue up to 50 years of age, with some decline being observed in older adulthood (Smit et al., 2012). A pronounced increase in long distance—frontal to occipital—synchronization, specifically in the alpha EEG band, was reported when comparing a group of children and adults (Srinivasan, 1999). More recently, Bathelt et al. (2013) used high-density EEG recordings combined with source reconstruction to demonstrate age-dependent increases in functional connectivity within wide-band frequency ranges from 2 to 5 years of age. In an attempt to establish a direct link between electromagnetic recordings of brain activity and the resting state networks identified in previous fMRI studies, inter-regional amplitude correlations were observed to increase continuously across childhood and adolescence, in multiple frequency bands (Schäfer et al., 2014). Similarly, an information theoretic analysis of EEG (Vakorin et al., 2011) provided evidence that the increased complexity of brain signals across infancy and childhood is related to greater integration of distributed neuronal populations. Although it is impossible to directly compare findings from fMRI and electrophysiological studies, given the sharp differences in signal origin (Horwitz, 2003; Singh, 2012), these disparate modalities may nonetheless reveal some shared topological characteristics of network development. Graph theory potentially provides a convenient mathematical framework for characterizing network topology and comparing network features across different recording modalities (Kaiser, 2011; Rubinov and Sporns, 2010; Stam and van Straaten, 2012). Graph theoretical methods have been increasingly applied to the study of human brain development to reveal the emergence of ordered, large-scale cerebral networks across ontogeny (Chu-Shore et al., 2011).

The present study

Our goals in the current study were to examine: (i) age-dependent differences in spontaneous EEG power spectral density and (ii) the development of band-limited functional brain network topology using weighted functional connectivity matrices. We focused on a large cross-sectional community sample of children between the ages of 7 to 11 years, grouped into one-year bands. This age range, encompassing early to late childhood, has been either under-sampled or collapsed and examined as a broad age group in many previous studies, despite the fact that it represents a critical developmental window that precedes the onset of adolescence. We simultaneously sought to address several methodological limitations of prior research examining EEG maturation. One major limitation of earlier work on age-related changes in spectral

EEG content is the reliance on canonical, wide frequency bands (see Cragg et al., 2011 for a notable exception). For example, investigators often adapt traditional frequency band definitions from the adult EEG literature and subsequently average spectral content over bins containing multiple Hz of neuronal activity. However, bands derived from the adult EEG literature may be inappropriate in developmental populations as indicated by previous work examining infants up to 4 years of age (Marshall et al., 2002). As a result of this strategy, it is possible to miss the spectral microstructure of intrinsic EEG activity that may be better captured by a continuous parsing of spectral content (Cragg et al., 2011). Here, we decomposed the EEG spectrum into a continuous range and used mass univariate statistical testing to explore maturational changes. Second, volume conduction is known to inflate estimates of EEG functional connectivity (Nunez and Srinivasan, 2006), particularly at short distances (<10 cm). Indeed, in pediatric populations inter-electrode distance accounts for over 50% of the variance in connectivity estimates (Barry et al., 2005). To overcome this limitation we quantified EEG functional connectivity using a metric that suppresses instantaneous synchrony arising due to linear signal mixing at the scalp (Palva and Palva, 2012), which effectively eliminates connectivity stemming from volume conduction. Finally, unlike traditional graph theoretical approaches to the study of functional brain network topology which apply thresholds to create binary (unweighted) networks, we employed methods from network science that use weighted links, thus minimizing the likelihood that our findings might be biased by the selection of relatively arbitrary thresholds (Newman, 2004).

Method

Participants

Participants were a subset drawn from a larger study of children recruited from the community. The inclusion criteria for children included being between the ages of 7 and 11 years. Exclusionary criteria were the presence of severe developmental or learning disabilities (e.g., autism) in children per parent report or parent symptoms of schizophrenia, alcohol or substance abuse or dependence within the last six months, or history of bipolar I disorder. Resting EEG data were available from a total of 276 children. After *Z*-scoring the average resting EEG spectrum across frequencies and electrode sites, 7 outliers (± 3 S.D. units) were identified and eliminated from further analyses (2 seven year olds, 2 eight year olds, 2 nine year olds and 1 ten year old) resulting in a total of 269 participants for all analyses. The final number of participants included across all five age groups was as follows: 61 seven year olds (29 females), 53 eight year olds (25 females), 52 nine year olds (30 females), 56 ten year olds (25 females), and 47 eleven year olds (16 females). Of the children included in our sample, 67.7% were Caucasian (13.8% African American) and the median family income ranged from $35,000 to $40,000. There were no significant differences across age groups in terms of children's sex, race, or family income (lowest $p = .47$).

Procedure

Potential participants were recruited from the community through a variety of means (e.g., television, newspaper and bus ads, flyers). Parents responding to the recruitment advertisements were initially screened over the phone to determine potential eligibility. Upon arrival to the laboratory, parents were asked to provide informed consent and children were asked to provide assent to be in the study. Next, participants were seated quietly in the experimental room and instructed to remain still with their eyes closed for a full minute. Although participants also completed an eyes-open condition, we sought to more carefully isolate spontaneous cortical activity by focusing specifically on eyes-closed recordings. This decision is consistent with recent recommendations that eyes-closed recordings provide a more appropriate method for capturing spontaneous brain function since eye opening leads to demonstrable changes in arousal state (Barry et al., 2007; van Diessen et al., in press) and passive fixation introduces cognitive load effects in addition to evoking neuronal entrainment at the refresh rate of monitor displays (Logothetis et al., 2009).

EEG recording

Continuous EEG was recorded using a custom cap and the BioSemi ActiveTwoBio system. Unreferenced EEG was digitized at 24-bit resolution with a sampling rate of 512 Hz. Recordings were taken from 34 sintered Ag/AgCl active scalp electrodes based on the International 10/20 system and evenly distributed across the head. Two additional electrodes were used in the study: an active Common Mode Sense (CMS) and a passive Driven Right Leg (DRL) electrode, located at the mid-line between C3 and CZ, and CZ and C4, respectively. Raw EEG was recorded relative to CMS. The CMS/DRL electrodes formed a loop that principally served as the ground for recordings through a feedback that subtracted the average potential of the subject (*i.e.,* the Common Mode voltage) to drive EEG recordings as close as possible to the "zero" ADC reference voltage in the AD-box (please see, http://www.biosemi.com/faq/cms&drl.htm for further details). The electrooculogram was recorded from four facial electrodes to capture vertical and horizontal eye movements that were subsequently used to aid visual inspection of the EEG time series.

EEG analysis and data reduction

Offline processing of EEG data was accomplished using a combination of EEGLAB (Delorme and Makeig, 2004) functions (for re-referencing, bandpass filtering and artifact rejection) and custom written, in-house MATLAB routines. After re-referencing the EEG data to Cz, a two-way least squares finite impulse response (FIR) filter was used to bandpass the time domain signal (low pass cut-off: 0.10 Hz, high pass cut-off: 35 Hz). Subsequently, visual inspection of eyes closed EEG data by trained observers was used to detect and remove segments contaminated by excessive noise or other gross artifacts (e.g., muscle movement, slow drift, line noise). A minimum of 30 seconds (s) of clean EEG data was considered necessary for inclusion in the final set of analyses reported in this paper. To ensure that there were no systematic differences in artifact-free epoch length as a function of age, we conducted pairwise contrasts for all of the age group comparisons. There were no group differences in the amount of artifact-free data that was retained for analysis, with the exception of a trend level ($p = 0.06$) effect for the eleven *vs.* seven years of age comparison (all other *p*s > 0.15). The mean duration of the artifact-free segments was well above 30 s for each age group ($M_{eleven} = 55.6$ s, $M_{ten} = 54.1$ s, $M_{nine} = 54.3$ s, $M_{eight} = 54.9$ s, $M_{seven} = 53.4$ s).

Power density analyses

The artifact-free time domain data from each cephalic electrode were detrended by removing the best straight-line fit and submitted to a frequency analysis using the Welch periodogram method with Hanning tapered windows of 2 s duration and 50% window overlap. Power spectral density (μV^2/Hz) was estimated for a continuous range from 0.5 to 30 Hz in steps of 0.50 Hz. We did not extend our analyses to frequencies higher than 30 Hz as initial visual inspection (prior to filtering) suggested very minimal contributions from those frequencies in the eyes-closed resting spectrum and we further wished to reduce the likelihood of contamination by electromyogenic artifacts. Prior to further analysis, spectra were transformed to decibel (dB) units in order to standardize individual differences in EEG amplitude. Relative power was calculated in percentage (%) values by expressing density within each 0.5 Hz bin as a fraction of total density within the 0.5–30 Hz range. In order to quantify an individual's peak alpha frequency, we used an automated peak detection algorithm that searched for the maximum 0.50 Hz bin falling within a narrow band (7–14 Hz) range.

Functional connectivity analyses

To minimize the contribution of volume conduction to functional connectivity, we opted to use a measure (the imaginary component of coherency) that is immune to artificial synchrony arising from linear signal mixing (Nolte et al., 2004; Palva and Palva, 2012). Under the assumption that the effects of volume conduction at the scalp are instantaneous (electrical fields travel at the speed of light), with no phase distortion, measures that exclusively quantify time lagged synchronization while suppressing zero millisecond phase lag relations can help separate true brain interactions from artificial synchrony (Cohen, 2014).

We quantified the absolute value of the imaginary part of a complex quantity, coherency (C_{xy}), where this complex value was defined at each specific frequency (f) as:

$$C_{xy}(f) = \frac{S_{xy}(f)}{\sqrt{S_{xx}(f)S_{yy}(f)}}$$

where S_{xy} is the cross power spectral density, while S_{xx} and S_{yy} are the power spectral densities of time series x and y, respectively. The spectral and cross-spectral densities were estimated using Welch's method, by equally dividing the artifact-free resting period into Hanning windows of 1 s duration (using longer windows risks introducing non-stationary activity and biasing functional connectivity estimates) with 50% overlap (see Bortel and Sovka, 2007). Isolating the imaginary component produces non-vanishing values only for time-lagged coupling, $0 < \theta\,(C_{xy}(f)) < 2\pi$. As indicated in Fig. 1, the imaginary component of coherency emphasized long-range functional connectivity while eliminating spurious connectivity estimates between spatially neighboring electrodes. Functional connectivity was estimated in the theta (4–7 Hz), alpha (8–13 Hz) and beta (14–30 Hz) wide-bands for all possible pairwise interactions of cephalic electrodes, leading to 33 x 33 weighted connectivity matrices for each individual participant. Note that in order to obtain reliable estimates of functional connectivity, we required that least four complete oscillatory cycles could fit within the 1 s periodogram window. Accordingly, the lower spectral edge being quantified was set at 4 Hz. There were several reasons for selecting wide frequency bands for functional connectivity analyses. Most importantly, time-lagged estimates of functional connectivity are highly prone to even minor non-stationarities in the frequency of neuronal oscillators (Cohen, 2015). For example, slight mismatches in peak frequency lead to a reduced ability to detect true oscillatory synchronization; as a result, using wider bands helps to minimize volatile fluctuations in connectivity estimates arising due to the natural non-stationarity of EEG epochs. Second, to ease the computational burden of calculating N × N matrices of network connectivity for each 0.5 Hz increment, we estimated functional connectivity using the dominant bands that we could qualitatively observe in our mass univariate analyses.

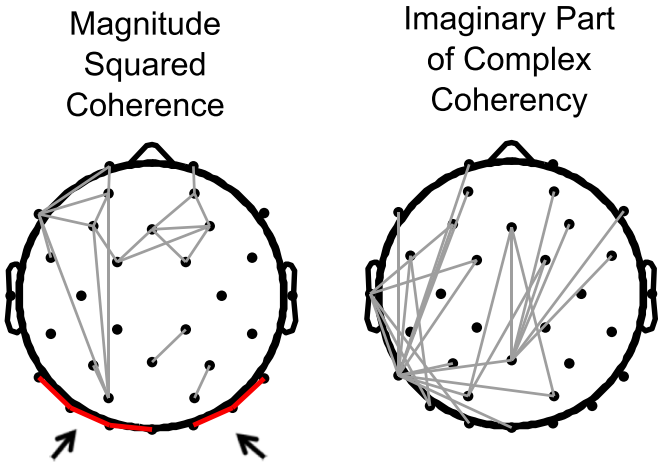

Fig. 1. A comparison of the traditional, magnitude squared coherence (left) and a phase-lagged index (*right*) of functional connectivity in the alpha-band (8–13 Hz) of the EEG from a randomly selected experimental participant. For each of the two measures, only connectivity values exceeding the 95th percentile are plotted topographically. The phase-lagged index was based on quantifying the imaginary portion of complex coherency. By using this method, inter-electrode coherence values having a 0 ms. phase lag with respect to each other are ignored and the only non-vanishing values appear for synchronous pairs having a time lag. Note that the traditional index is sensitive to high coherence values for spatially neighboring electrodes (e.g., the connection links highlighted in red and indicated by arrows) which likely reflects artificial synchrony arising due to volume conduction.

Subsequently, topological network measures were calculated on the basis of the N × N (weighted) adjacency matrices using functions from the Python package, NetworkX. For each adjacency matrix, we calculated the characteristic path length and the modularity (also called the Q-metric) as the topological metrics of the network. Characteristic path length is the arithmetic average of shortest path lengths between all pairs of nodes in the network. While this metric becomes infinite if there are disconnected components within the network, our data are weighted adjacency matrices where all node pairs are connected with some positive link weights. When calculating a path length, the link weights (functional connectivity strengths) are replaced by their reciprocals so that a stronger connectivity is mapped to a shorter path length. Therefore, shorter characteristic path length implies stronger overall functional connectivity in the network (Rubinov and Sporns, 2010).

A modularity of a network measures how well the network topology can be captured in several distinct groups of nodes (communities). It is defined as

$$Q = \frac{|E_{in}| - |E_{in\_r}|}{|E|},$$

where $|E|$ is the total number of links, $|E_{in}|$ the number of links that connect nodes within groups, and $|E_{in\_r}|$ is the number of such within-group links that would be expected if the network topology were randomized. For weighted networks like those in our data, the number of links is replaced by the total link weights of links. We used the Louvain method (Blondel et al., 2008) to find the optimal community structure, on which the maximal modularity is heuristically calculated.

In addition, we measured how homogeneous the nodes' strengths (*i.e.*, the sum of link weights connected to a particular node) are within a network, by measuring their Shannon entropy as

$$H = -\sum_{i=1}^{33} P_i \log_2 P_i$$

where i is the node (in this case, electrode) ($i = 1, 2, \ldots 33$) and $P_i = \frac{D_i}{\sum_{j=1}^{33} D_j}$ with D_i (or D_j) being the strength of node i (or j). This metric, which we call "strength homogeneity" takes its maximal value $\log_2(33) = 5.04$ if all nodes have the same strength, *i.e.*, the strength distribution is perfectly homogenous. Conversely, it takes its minimal value, 0, if only one node has all of the strength while others have zero strength (which would never occur with empirical data). Therefore this metric captures how evenly the connectivity is distributed among nodes.

Statistical analyses

Since we wished to avoid averaging spectral density across wide-band bins defined *a priori*, we adopted a mass univariate approach to test for age-related changes in EEG power. To detect reliable spectral and spatial differences in EEG content as a function of age, we submitted the power density data to an independent samples, two-tailed permutation test based on the t_{max} statistic (Blair and Karniski, 1993; Groppe et al., 2011) using a family-wise alpha level of 0.05, effectively controlling for the inflation of Type I error rates. All frequency bins between

0.5 and 30 Hz at all 33 cephalic electrodes were included in the test (*i.e.*, 754 total comparisons). We did not test for differences in frequencies exceeding 30 Hz due to the nature of band-pass filtering and since, consistent with other EEG studies, our sample exhibited minimal spectral density for frequencies in that range. Adopting a Monte Carlo approach, we used 1000 random between-participant permutations of the data to empirically approximate the distribution of the null hypothesis (*i.e.*, no difference between age groups) for the contrasts of interest. The number of random permutations was based on previous suggestions in the literature (Manly, 1997). Based on this estimate, critical *t*-scores were derived and any between-group differences in the original data that exceeded the t_{max} statistic were deemed reliable. Statistical testing of the alpha peak frequency and graph theory metrics similarly used an approximative K-sample one-way randomization tests with 1000 random between-participant permutations of the data. All statistical analyses were performed using MATLAB and R (R Development Core Team, 2008).

Results

Developmental shifts in absolute EEG spectral density

As highlighted by the statistical saliency maps (see Fig. 2), there were significant ($p_{perm} < 0.05$) age-related changes in absolute EEG spectral density. Specifically, compared to the 11 year olds, the 7 (Fig. 2 inset, *top left*), 8 (Fig. 2 inset, *top right*), 9 (Fig. 2 inset, *bottom left*) and 10 (Fig. 2 inset, *bottom right*) year olds all exhibited increased density of slow wave power from about 0.5 Hz extending to the border between the traditional alpha$_1$ and alpha$_2$ EEG bands around 9 to 10 Hz. Interestingly, by 10 years of age, the spectral extent of this effect had contracted and appeared more confined to the traditional theta-band range (~4 to 7 Hz). The remaining age contrasts are provided in the Supplementary Materials section (Fig. S1). There was no indication of spatial specificity to this effect, as the age-related decline in slow power was evident across all of the major regions from frontal to occipital.

To conduct a more fine grained chronological analysis we averaged a wide swath of slow wave spectral density encompassing the traditional delta and theta bandwidths (0.5 to 7 Hz) and pooled the data for separate regional electrode clusters along a posterior–anterior continuum (occipital, parietal, central and frontal). We then related this to a continuous measure of age, measured in years. The results of regionally specific linear fit models using continuous age as a predictor of slow wave power density are visualized in Fig. 3. To ensure the robustness of these effects we performed a permutation test of the association between continuous age and regional slow wave power density using approximative Spearman correlation tests with 9,999 replications. The results indicated significant negative correlations across all regional electrode clusters (all $ps < 4 \times 10^{-11}$).

A second trend evident in terms of our mass univariate spatio-spectral analyses concerns the age-related decrease in high frequency EEG spectral density ($p_{perm} < 0.05$), roughly corresponding to an

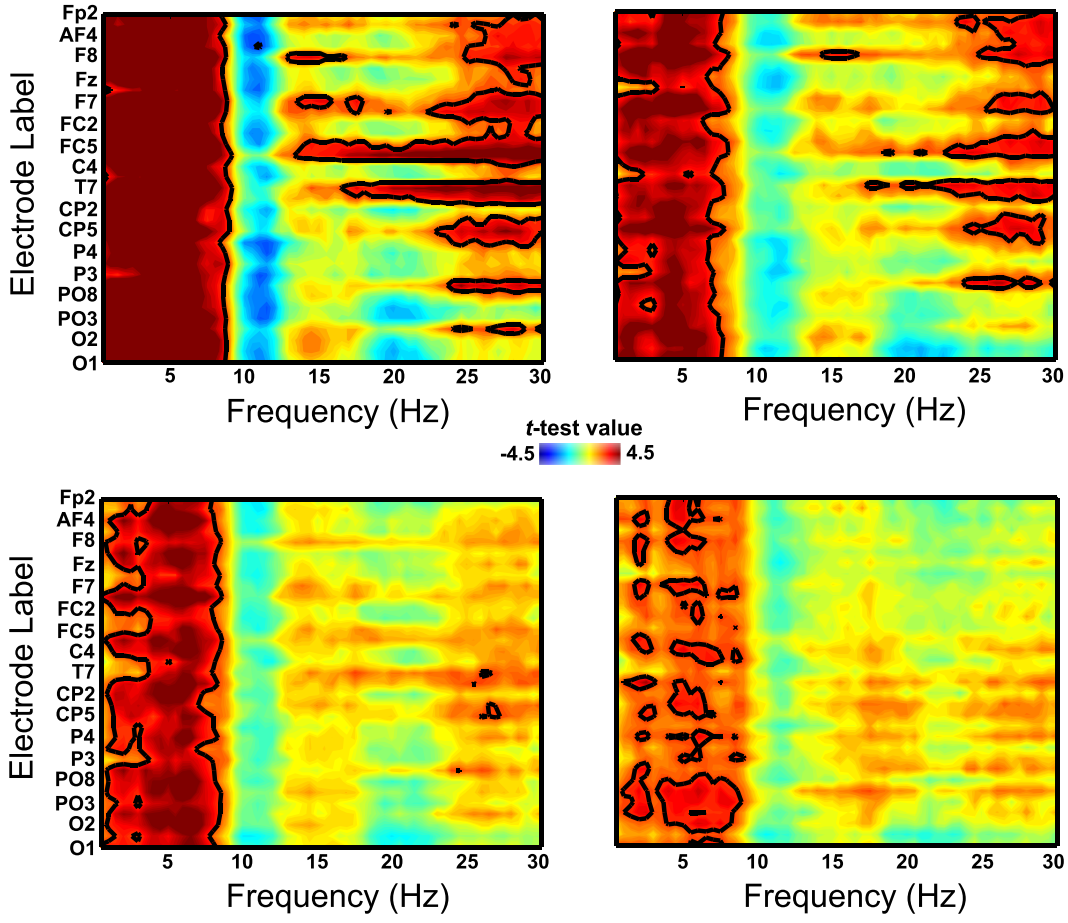

Fig. 2. Spatio-spectral saliency maps for the 7 *vs.* 11 year old (top left), 8 *vs.* 11 year old (top *right*), 9 *vs.* 11 year old (*bottom left*) and 10 *vs.* 11 year old (*bottom right*) mass univariate analyses using a t_{max} Monte Carlo method (with 1000 random between-subject data permutations). The dependent variable of interest is absolute spectral density. Regions outlined in black highlight the electrodes and frequencies that reached statistical significance using a permutation-controlled familywise alpha level of 0.05. Hot colors denote increased power in the comparison groups relative to the 11 year olds while cool colors indicate the opposite. Note that the electrodes are arranged in order from the most anterior (top portion of the y-axis) to the most posterior (bottom portion of the y-axis); because of space constraints, not all electrode labels are shown.

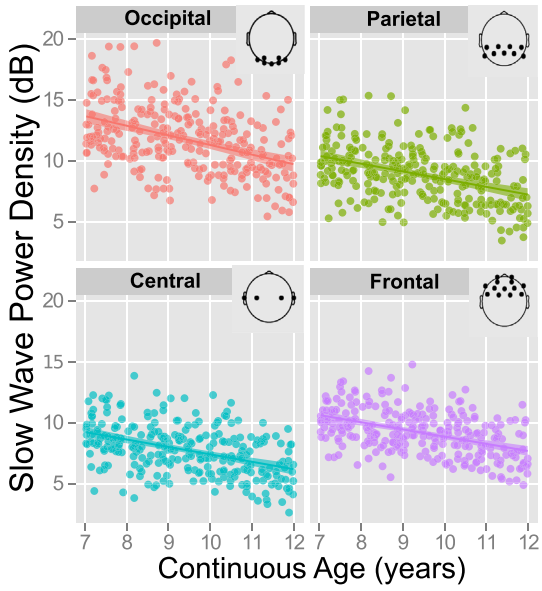

Fig. 3. Regional scatter plots and regression lines using continuous chronological age to predict variability in absolute slow wave (0.5–7 Hz) EEG spectral density is shown across four separate electrode clusters.

expanded beta band (~14 to 30 Hz). In contrast to the slow wave power findings, this effect seemed more regionally restricted to fronto-central sites. Contrasts of the 9 and 10 year old age groups against the 11 year olds no longer revealed significant effects in this high frequency range suggesting a slightly different EEG maturational trend compared to the slow wave spectral density range.

Developmental shifts in relative EEG spectral density

Our findings in terms of relative spectral EEG density changes across the age groups are illustrated in Fig. 4. The main advantage of computing relative spectral density, compared to absolute spectral density, is that it helps to control for individual differences in such physical parameters as skull thickness and cell density which can contribute to variability in estimates of absolute spectral density recorded at the scalp. Consistent with earlier findings, we observed age-related increases ($p_{perm} < 0.05$) in the relative concentration of high frequency EEG density when contrasting 11 year olds with 7 (Fig. 4 inset, *top left*) and 8 (Fig. 4 inset, *top right*) year olds. This increase in relative spectral density largely encompassed the traditional alpha$_2$ sub-bandwidth (~10 to 13 Hz) with some encroachment into the beta range (>14 Hz) and they largely disappeared when contrasting the older age groups (9 and 10 year olds). The remaining contrasts for relative spectral density are highlighted in Supplementary Materials (see Fig. S1).

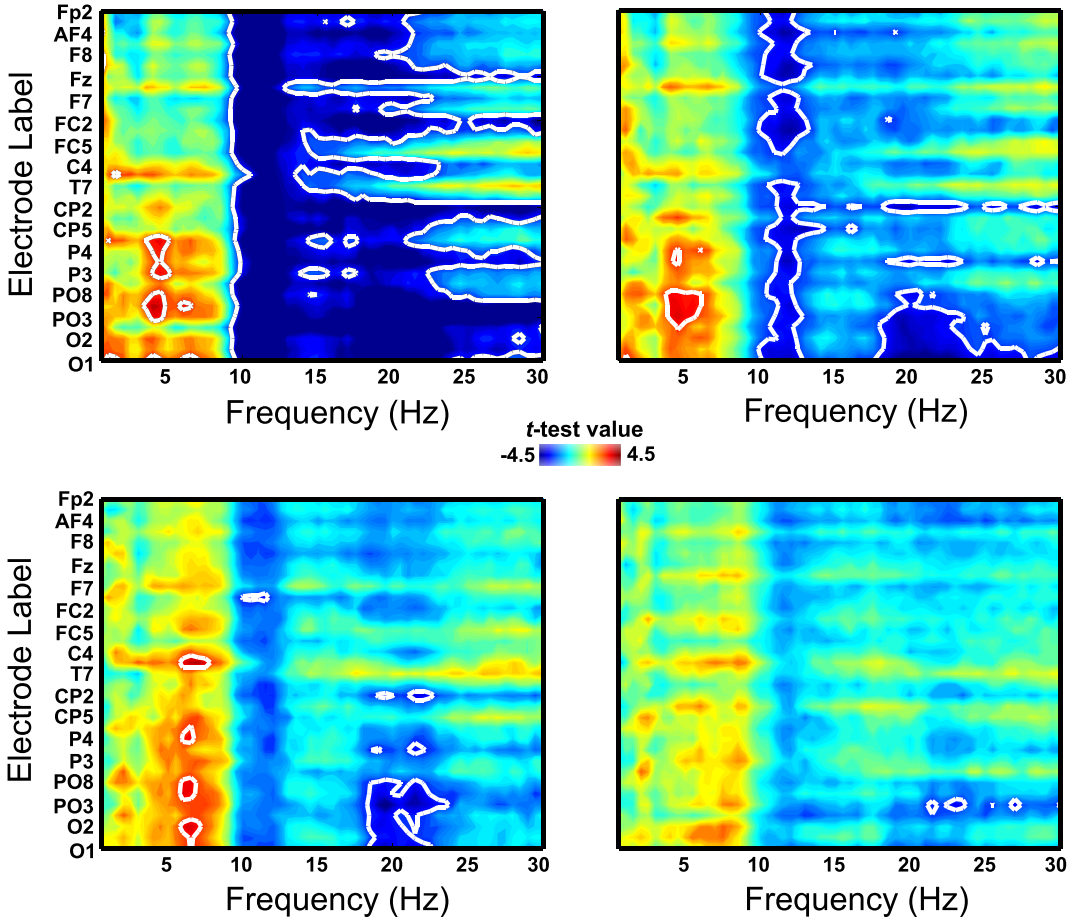

Fig. 4. Spatio-spectral saliency maps for the 7 *vs.* 11 year old (top left), 8 *vs.* 11 year old (top *right*), 9 *vs.* 11 year old (*bottom left*) and 10 *vs.* 11 year old (*bottom right*) mass univariate analyses using a t_{max} Monte Carlo method (with 1000 random between-subject data permutations). The dependent variable of interest was *relative* spectral density. Regions outlined in white highlight the electrodes and frequencies that reached statistical significance using a permutation-controlled familywise alpha level of 0.05. Hot colors denote increased power in the comparison groups relative to the 11 year olds while cool colors indicate the opposite. Note that the electrodes are arranged in order from the most anterior (top portion of the y-axis) to the most posterior (bottom portion of the y-axis); because of space constraints, not all electrode labels are shown.

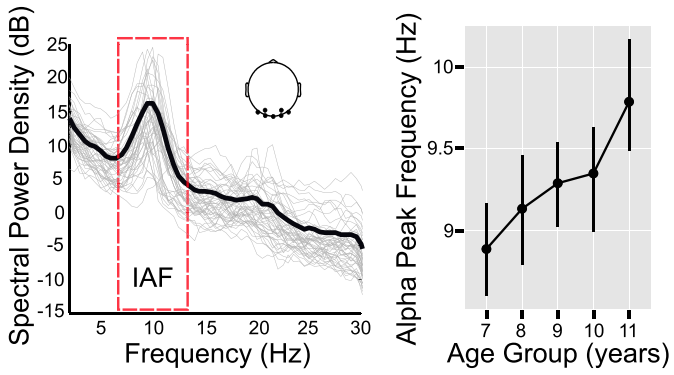

Fig. 5. The eyes-closed EEG spectrum (left) for a cluster of posterior electrodes (highlighted in the 2D topographic inset) is shown both for single subjects (thin gray lines) and the overall group mean (bold black line) in the group of 11 year olds. Note the variation in individual alpha frequency (IAF). An automated peak detection algorithm was used to identify each individual's peak within the IAF range (7–14 Hz). The mean alpha peak frequency across the five age groups is depicted on the right, indicating a progressive linear increase in the peak frequency across age. Error bars depict 95% confidence intervals estimated using bootstrapping with 1000 random iterations.

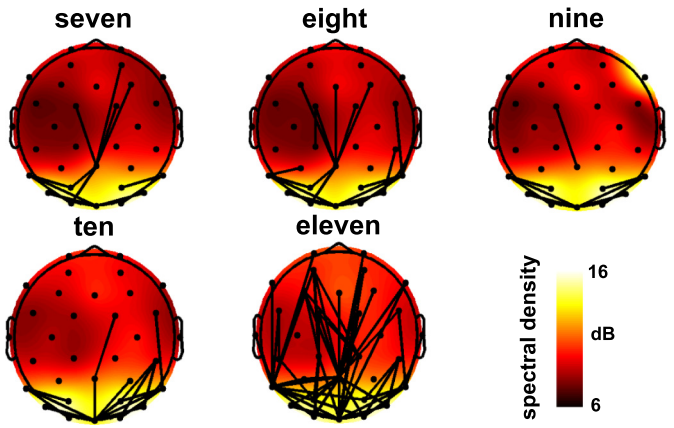

Fig. 6. Functional alpha-band (8–13 Hz) connectivity links that exceeded a threshold set at the 95th percentile of connectivity values (across all subjects) are depicted for visualization purposes, superimposed over spherical spline interpolated topographic maps that indicate the distribution of alpha-band power spectral density. Note that thresholding was applied here purely for visualization purposes; all statistical tests reported in the paper were conducted on graph theoretic measures derived from weighted connectivity networks.

Developmental shifts in alpha peak frequency

There was a significant difference ($p_{perm} < 3 \times 10^{-16}$) among the age groups in the alpha peak frequency. As highlighted in Fig. 5, there was a linear increase from a mean value of 8.89 Hz at 7 years of age to 9.79 Hz at 11 years of age. The alpha peak frequency in the group of 11 year olds was higher than in all of the other age groups. The results of post-hoc pairwise *t*-contrasts (with False Discovery Rate [FDR] correction) are provided in Table 1.

Developmental shifts in EEG network organization

Theta-band

There were no effects of age on the graph theoretic indices of theta-band (4–7 Hz) EEG network organization (all *ps* > 0.19).

Alpha-band

As illustrated in Fig. 6, there was an age-dependent increase in the strength of long-range functional connectivity within the alpha band (8–13 Hz) that culminated with the most densely connected networks in the group of 11 year olds. This visual impression was confirmed by statistical analyses which revealed significant age effects on alpha-band network organization for each of the three graph theoretic measures under consideration including characteristic path length ($p_{perm} = 0.02$), modularity index (Q-metric) ($p_{perm} < 2.2 \times 10^{-16}$) and strength homogeneity ($p_{perm} < 3 \times 10^{-16}$). Table 2 lists the FDR corrected probability values of all pairwise *t*-contrasts. There was a strong linear trend apparent in the data, with shorter path lengths, decreased modularity and decreased network homogeneity across chronological age (see Fig. 7).

Beta-band

There were no effects of age on the graph theoretic indices of beta-band (14–30 Hz) EEG network organization (all *ps* > 0.23).

Exploratory analyses of sex differences

Since our sample included children in the pre-adolescent stage of development we had no explicit hypotheses about sex. Nevertheless, to examine whether sex moderated any of the age-related effects observed in our mass univariate analyses we conducted a set of follow-up factorial ANOVAs (using Type III Sums of Squares) with the between-subject factors of Age and Sex and the within-subject factor of Region (posterior, parietal, central and frontal). Instead of relying on traditional, *a priori* defined bands we focused primarily on the spectral regions that revealed significant age effects in our permutation controlled analyses. Thus, we created regional means of slow wave (0.5 to 7 Hz) and high frequency (14 to 30 Hz) bands. The only significant findings in terms of sex were differences in absolute spectral density. Specifically, there were sex differences in slow wave (0.5 to 7 Hz) [$F_{(1,259)} = 5.48$, $p = 0.02$] and high frequency (14 to 30 Hz) [$F_{(1,259)} = 15.81$, $p < 0.001$] bandwidths, with males exhibiting less absolute spectral density within each of these frequency ranges. None of the other Age × Sex

Table 1
Probability values (FDR corrected) for individual alpha peak frequency contrasts.

Contrast	Alpha peak
7 *vs.* 8	0.25
7 *vs.* 9	**0.02***
7 *vs.* 10	**0.02***
7 *vs.* 11	<**0.001****
8 *vs.* 9	0.41
8 *vs.* 10	0.32
8 *vs.* 11	**0.004****
9 *vs.* 10	0.72
9 *vs.* 11	**0.01***
10 *vs.* 11	**0.03***

Note: * $p < 0.05$; ** $p < 0.01$.

Table 2
Probability values (FDR corrected) for contrasts of characteristic path length (CPL), modularity index and strength of homogeneity in alpha-band EEG networks.

Contrast	CPL	Modularity	Strength homogeneity
7 *vs.* 8	0.97	0.95	0.62
7 *vs.* 9	0.32	0.95	0.62
7 *vs.* 10	0.09^{+}	0.59	0.31
7 *vs.* 11	**0.02***	<**0.01****	<**0.01****
8 *vs.* 9	0.38	0.95	0.99
8 *vs.* 10	0.14	0.63	0.62
8 *vs.* 11	**0.04***	**0.01***	**0.03***
9 *vs.* 10	0.32	0.59	0.62
9 *vs.* 11	0.06^{+}	<**0.01****	**0.01***
10 *vs.* 11	0.32	**0.05***	0.07^{+}

Note: * $p < 0.05$; ** $p < 0.01$.

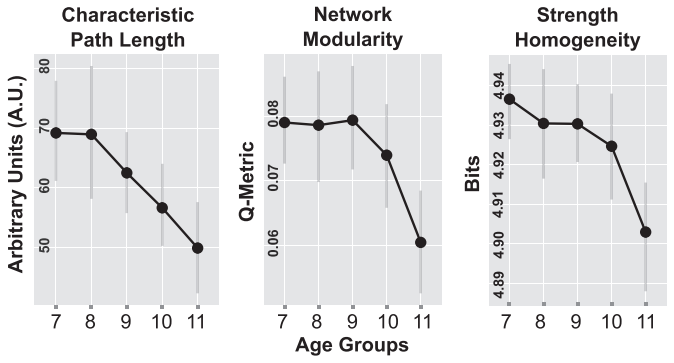

Fig. 7. Graph theoretic metrics estimated on the basis of a weighted alpha-band (8–13 Hz) EEG functional connectivity networks. Error bars depict 95% confidence intervals estimated using bootstrapping with 1000 random iterations.

interactions were significant for analyses focused on relative spectral density, alpha peak frequency and graph theoretic indices (all *ps* > 0.23).

Discussion

Our study explored the maturation of spectral density and long range synchronization of cerebral electric fields from early to late childhood in a large, cross-sectional community sample. Crucially, rather than averaging across this age range, as was often done in previous studies comparing children to adolescents and adults, we examined brain maturation in one year windows. We utilized several novel approaches in our investigation including performing a more fine grained analysis of spectral density maturation (in contrast to classic broad bands), employing a phase-lagged index of brain functional connectivity to estimate resting EEG cortical networks and applying a topological network analysis to weighted rather than binary brain connectivity matrices as traditionally implemented in the developmental literature.

Consistent with many previous studies (Segalowitz et al., 2010; Uhlhaas et al., 2010), we discovered age-related declines in the absolute spectral density of low frequency EEG oscillations. This complements existing research showing that rates of cerebral glucose utilization (Chugani, 1998), gray matter density (Giedd et al., 1999; Gogtay et al., 2004; Whitford et al., 2007) and spontaneous slow fluctuations of BOLD activity (Lüchinger et al., 2012) all decrease with age, supporting the theory that the brain undergoes extensive maturational reorganization that is powerfully driven by "regressive" mechanisms where initial synaptic overproduction is followed by selective elimination and ultimately stabilization (Feinberg and Campbell, 2010). The results of our mass univariate analyses suggest that the spectral locus of brain electric maturation does not honor traditional separation of classical delta and theta bands, but rather extends in a spatially diffuse manner to the boundary between the $alpha_1$ and $alpha_2$ bandwidths. To a lesser extent, the age dependent decrease of absolute EEG spectral density was also present for higher frequencies (above 14 Hz), in close correspondence with recent findings of EEG maturation into the second and third decades of life (Cragg et al., 2011; Kurth et al., 2010; Michels et al., 2013; Rodríguez-Martínez et al., 2015; Whitford et al., 2007).

On the basis of a statistical relation between reductions in cortical gray matter density and absolute EEG spectral power, particularly in the slow wave range, (Buchmann et al., 2011; Whitford et al., 2007), a plausible hypothesis is that cortical neuropil reduction actually drives decreased EEG power since the latter reflects the summed membrane potentials of pyramidal cells (Uhlhaas et al., 2010). However, it remains possible that these two phenomena (reductions in gray matter thickness and EEG spectral density) represent common correlates of cortical development without being causally linked. There are several observations that collectively argue against a direct causal link between reductions in gray matter volume and EEG spectral density (Lüchinger et al., 2012). First, developmental changes in gray matter thickness are regionally specific, exhibiting different longitudinal schedules across cortical lobes (Giedd, 2004; Giedd et al., 1999; Gogtay et al., 2004; Shaw et al., 2008). By contrast, we did not observe any topographic specificity in the reduction of low frequency EEG across age groups. Instead, there was a robust negative correlation between chronological age and spectral density across all of the major cortical lobes, consistent with other EEG studies (Cragg et al., 2011; Lüchinger et al., 2012; Whitford et al., 2007). Second, evidence from longitudinal studies of NREM sleep EEG suggests a slightly different maturational trajectory with relatively little changes in delta band power between 9 and 11 years age, followed by precipitous declines between 11 and 16 years of age (Campbell and Feinberg, 2009). This seems to suggest that the developmental timing of slow wave decline is partially state-dependent, which is not consistent with the hypothesis that EEG power reduction primarily reflects structural (volumetric) alterations.

An alternative explanation is that the spectral density of slow wave activity in resting state EEG is largely determined by resonant thalamo-cortical loops. Using a combination of *in vitro* and *in vivo* findings, Llinás et al. (2005) have advanced a model in which the intrinsic membrane electrophysiology of thalamic relay cells spreads to zones of cortex via recurrent projections that effectively entrain large neuronal populations. Specifically, during membrane hyperpolarization thalamic relay cells switch to a low frequency burst mode of firing that globally slows cortical electric rhythms, leading to increased delta and theta spectral density in surface recordings of electromagnetic brain function (Llinás et al., 1999, 2005; see also Hughes and John, 1999). Interestingly, this model also predicts that low frequency oscillations in thalamo-cortical relay neurons lead to a disinhibitory "edge effect" in which there is a rebound that involves simultaneously increased spectral density of beta and gamma rhythms (Llinás et al., 2005), similar to what we observed in terms of our absolute power findings. The combination of excess delta and theta power, a slowing of the dominant alpha peak and a secondary increase of high frequency oscillations have been reported in a number of neurological and psychiatric conditions (Llinás et al., 1999; Schulman et al., 2011). Although this specific type of thalamo-cortical "dysrhythmia" has largely been discussed in the context of calcium channelopathies, a variety of mechanisms that increase low frequency thalamic rhythmicity are predicted to produce similar outcomes (Llinás et al., 2005). Recent findings using simultaneous EEG-fMRI recordings, have discovered marked differences in thalamo-cortical coupling between children and adolescents suggesting that it is possible to link typical brain maturation with other global states involving similar spectral signatures (Lüchinger et al., 2012). Since thalamic relay cells project to cortical regions globally, this may account for the lack of topographic specificity in our EEG findings.

In terms of relative spectra, our findings are consistent with previous developmental studies in suggesting a redistribution favoring higher frequency alpha and beta-band activity in older children (Bell and Wolfe, 2008; Cragg et al., 2011). However, these differences were less drastic compared to the reductions in absolute power—the group of eleven year olds did not differ appreciably when compared with the nine and ten year olds. By comparison, the peak of the dominant alpha rhythm continued to increase across age groups, spanning nearly an entire 1 Hz shift when contrasting the seven and eleven year old children and remained significant when comparing ten and eleven year olds (see also Cragg et al., 2011). Axonal myelination and the integrity of white matter pathways have been suggested to underlie alpha peak frequency shifts (Segalowitz et al., 2010; Valdés-Hernández et al., 2010).

A striking finding from structural magnetic resonance imaging of the developing cortex concerns the linear increase in white matter density across age (reviewed in Casey et al., 2005 and Giedd, 2004). In addition to the peak of the oscillatory alpha rhythm, another electrophysiological marker of white matter maturation is found in patterns of long range neuronal synchronization (Chu et al., 2015; Teipel et al., 2009; Thatcher et al., 1998). Previous evidence indicates that long

range EEG coherence increases across age (Barry et al., 2004), particularly in the alpha-band frequency range (Ghemlin et al., 2011; Schäfer et al., 2014; Srinivasan, 1999). One major limitation in inferring functional connectivity on the basis of extracranially recorded electric signals concerns the confounding effects of volume conduction, especially at short electrode distances (Barry et al., 2005). Accordingly, we implemented a measure of functional connectivity (the imaginary component of complex coherency) that removes zero phase lag relations emerging from volume conduction, while emphasizing more long range brain interactions. Consistent with some of the earlier reports utilizing much smaller sample sizes (Barry et al., 2004, but see Thatcher et al., 2008), our findings demonstrate that the oldest age group exhibited the densest patterns of functional connectivity across distant cortical regions, specifically within the alpha band. These findings are also broadly consistent with one of the more replicable fMRI results involving a trend toward increased integration among distant neural networks (Betzel et al., 2014; Fair et al., 2007, 2009; Supekar et al., 2009). Different imaging modalities have unique sensitivities for capturing phase-based *vs.* amplitude-based intrinsic coupling modes (Engel et al., 2013), and it remains to be determined how these distinct types of networks compare to each other (Schäfer et al., 2014).

On the basis of our network analyses, we can conclude that from early to late childhood, alpha-band electrocortical connectivity becomes more integrated (shorter characteristic path length), less functionally segregated (reduced modularity) and more spatially variable (less homogenous). One consequence of cortical networks with increased global integration appears to be their capacity to support a greater repertoire of functional cortical states (McIntosh et al., 2008; Vakorin et al., 2011, 2013). Indeed, in our data, older children exhibited functional alpha networks that were less spatially homogenous compared to those of younger children. Increased efficiency and variability of cortical states are related to improved performance on task-based measures, ranging from simple reaction time (McIntosh et al., 2008) to more complex indices of intellectual performance (van den Heuvel et al., 2009).

The age-related reductions in characteristic path lengths reported here are consistent with recent data from high density EEG recordings employing cortical source reconstruction analyses (Bathelt et al., 2013), as well as fMRI studies of resting state cortical networks (Vértes and Bullmore, 2015). Although there is only partial overlap between structural and functional brain networks (Damoiseaux and Greicius, 2009), it is interesting to note that our results also align with those demonstrating reduced characteristic path lengths and modularity from 12 to 30 years of age on the basis of structural cortical connections (Dennis et al., 2013).

We should also note, however, our network findings are partially in conflict with previous EEG studies demonstrating that path lengths and clustering both increase across development (Boersma et al., 2011) peaking around 18 years of age (Smit et al., 2012). There are a number of methodological reasons that might account for these inconsistencies. First, different metrics of EEG functional connectivity were employed: we used zero phase lag removed coherency, while the other studies calculated synchronization likelihood (Boersma et al., 2011; Smit et al., 2012), a non-linear measure of brain connectivity that depends on time delayed embedding of neural signals. Phase-lagged indices of functional connectivity, which are primarily sensitive to more long range links, may de-emphasize clustering/modularity of functional brain networks. Second, at least one of the previous studies (Smit et al., 2012) used thresholding procedures to binarize the networks, while we applied network analyses to weighted connectivity matrices, which provides a more continuous approach to quantifying topology.

Conclusions

Overall, we demonstrated considerable differences in the spontaneous EEG spectrum as a function of age, from early to late childhood. The globally distributed reductions of absolute EEG spectral density—especially in the slow wave range—represented perhaps the most salient manifestations of neuronal maturation. Consistent with extant theoretical proposals (e.g., Stevens, 2009) reduced amplitude of brain activity seems to be accompanied by reorganization and refinement of long range functional connectivity. In particular, even after accounting for the effects of volume conduction on brain electric signals, the density and spatial variability of alpha-band cortical networks increased in late childhood—this trend likely continues to mature into young adulthood (Uhlhaas et al., 2010). Taken together, these findings are consistent with evidence demonstrating that the maturing brain is characterized by an enhanced ability to maintain phase synchronized brain oscillations within specific frequency ranges (Ehlers et al., 2014; Poulsen et al., 2009; Uhlhaas et al., 2009). The ability to sustain precise patterns of neuronal coordination (*i.e.*, more precisely "tuned" brain networks), even among distant cortical areas, likely expands the repertoire of functional cortical states and increases information integration within the brain (Vakorin et al., 2011), which ultimately may underlie ontogenetic changes in cognitive function (Casey et al., 2005). Although we used a symmetric measure of functional brain connectivity, in the future this can be supplemented with effective connectivity analyses to indicate directional reversals in cortical information flow across different age groups (Michels et al., 2013). Moreover, it may be of interest to capture dynamic functional connectivity, fluctuating on varying time scales.

Supplementary data to this article can be found online at http://dx.doi.org/10.1016/j.neuroimage.2015.06.013.

References

Arieli, A., Sterkin, A., Grinvald, A., Aertsen, A., 1996. Dynamics of ongoing activity: explanation of the large variability in evoked cortical responses. Science 273, 1868–1871.

Barry, R.J., Clarke, A.R., McCarthy, R., Selikowitz, M., Johnstone, S.J., Rushby, J.A., 2004. Age and gender effects in EEG coherence: I. Developmental trends in normal children. Clin. Neurophysiol. 115, 2252–2258.

Barry, R.J., Clarke, A.R., McCarthy, R., Selikowitz, M., 2005. Adjusting EEG coherence for inter-electrode distance effects: an exploration in normal children. Int. J. Psychophysiol. 55, 313–321.

Barry, R.J., Clarke, A.R., Johnstone, S.J., Magee, C.A., Rushby, J.A., 2007. EEG differences between eyes-closed and eyes-open resting conditions. Clin. Neurophysiol. 118, 2765–2773.

Bathelt, J., O'Reilly, H., Clayden, J.D., Cross, J.H., de Haan, M., 2013. Functional brain network organisation of children between 2 and 5 years derived from reconstructed activity of cortical sources of high-density EEG recordings. NeuroImage 82, 595–604.

Becker, R., Reinacher, M., Freyer, F., Villringer, A., Ritter, P., 2011. How ongoing neuronal oscillations account for evoked fMRI variability. J. Neurosci. 31, 11016–11027.

Bell, M.A., Wolfe, C.D., 2008. The use of the electroencephalogram in research on cognitive development. In: Schmidt, L.A., Segalowitz, S.J. (Eds.), Developmental psychophysiology: theory, systems, and methods. Cambridge University Press, New York, NY, pp. 150–172.

Betzel, R.F., Erickson, M.A., Abell, M., O'Donnell, B.F., Hetrick, W.P., Sporns, O., 2012. Synchronization dynamics and evidence for a repertoire of network states in resting EEG. Front. Comput. Neurosci. 6, 74.

Betzel, R.F., Byrge, L., He, Y., Goni, J., Zuo, X.-N., Sporns, O., 2014. Changes in structural and functional connectivity among resting-state networks across the human lifespan. NeuroImage 102, 345–357.

Blair, R.C., Karniski, W., 1993. An alternative method for significance testing of waveform difference potentials. Psychophysiology 30, 518–524.

Blondel, V.D., Guillaume, J.-L., Lambiotte, R., Lefebvre, E., 2008. Fast unfolding of communities in large networks. J. Stat. Mech. 2008, P10008.

Boersma, M., Smit, D.J.A., de Bie, H.M.A., Van Baal, G.C.M., Boomsma, D.I., de Geus, E.J.C., et al., 2011. Network analysis of resting state EEG in the developing young brain: structure comes with maturation. Hum. Brain Mapp. 32, 413–425.

Bortel, R., Sovka, P., 2007. Approximation of statistical distribution of magnitude squared coherence estimated with segment overlapping. Signal Process. 87, 1100–1117.

Buchmann, A., Ringli, M., Kurth, S., Schaerer, M., Geiger, A., Jenni, O.G., Huber, R., 2011. EEG sleep slow-wave activity as a mirror of cortical maturation. Cereb. Cortex 21, 607–615.

Campbell, I.G., Feinberg, I., 2009. Longitudinal trajectories of non-rapid eye movement delta and theta EEG as indicators of adolescent brain maturation. Proc. Natl. Acad. Sci. U. S. A. 106, 5177–5180.

Casey, B.J., Tottenham, N., Liston, C., Durston, S., 2005. Imaging the developing brain: what have we learned about cognitive development? Trends Cogn. Sci. 9, 104–110.

Chiang, A.K.I., Rennie, C.J., Robinson, P.A., van Albada, S.J., Kerr, C.C., 2011. Age trends and sex differences of alpha rhythms including split alpha peaks. Clin. Neurophysiol. 122, 1505–1517.

Chu, C.J., Tanaka, N., Diaz, J., Edlow, B.L., Wu, O., Hämäläinen, M., et al., 2015. EEG functional connectivity is partially predicted by underlying white matter connectivity. Neuroimage 108, 23–33.

Chugani, H.T., 1998. A critical period of brain development: studies of cerebral glucose utilization with PET. Prev. Med. 27, 184–188.
Chu-Shore, C.J., Kramer, M.A., Bianchi, M.T., Caviness, V.S., Cash, S.S., 2011. Network analysis: applications for the developing brain. J. Child Neurol. 26, 488–500.
Cohen, M.X., 2014. Analyzing Neural Time Series Data: Theory and Practice. The MIT Press.
Cohen, M.X., 2015. Effects of time lag and frequency matching on phase-based connectivity. J. Neurosci. Methods 250, 137–146.
Cragg, L., Kovacevic, N., McIntosh, A.R., Poulsen, C., Martinu, K., Leonard, G., Paus, T., 2011. Maturation of EEG power spectra in early adolescence: a longitudinal study. Dev. Sci. 14, 935–943.
Damoiseaux, J.S., Greicius, M.D., 2009. Greater than the sum of its parts: a review of studies combining structural and resting-state functional connectivity. Brain Struct. Funct. 213, 525–533.
Deco, G., Jirsa, V., McIntosh, A.R., 2011. Emerging concepts for the dynamical organization of resting-state activity in the brain. Nat. Rev. Neurosci. 12, 43–56.
Deco, G., Jirsa, V., McIntosh, A.R., 2013. Resting brains never rest: computational insights into potential cognitive architectures. Trends Neurosci. 36, 268–274.
Delorme, A., Makeig, S., 2004. EEGLAB: an open source toolbox for analysis of single-trial EEG dynamics. J. Neurosci. Methods 134, 9–21.
Dennis, E.L., Jahanshad, N., McMahon, K.L., de Zubicaray, G.I., Martin, N.G., Hickie, I.B., et al., 2013. Development of brain structural connectivity between ages 12 and 30: a 4-tesla diffusion imaging study in 439 adolescents and adults. NeuroImage 64, 671–684.
Dosenbach, N.U.F., Nardos, B., Cohen, A.L., Fair, D.A., Power, J.D., Church, J.A., et al., 2010. Prediction of individual brain maturity using fMRI. Science 329, 1358–1361.
Dustman, R.E., Shearer, D.E., Emerson, R.Y., 1999. Life-span changes in EEG spectral amplitude, amplitude variability and mean frequency. Clin. Neurophysiol. 110, 1399–1409.
Ehlers, C.L., Wills, D.N., Desikan, A., Phillips, E., Havstad, J., 2014. Decreases in energy and increases in phase locking of event-related oscillations to auditory stimuli occur during adolescence in human and rodent brain. Dev. Neurosci. 36, 175–195.
Engel, A.K., Gerloff, C., Hilgetag, C.C., Nolte, G., 2013. Intrinsic coupling modes: multiscale interactions in ongoing brain activity. Neuron 80, 867–886.
Fair, D.A., Dosenbach, N.U.F., Church, J.A., Cohen, A.L., Brahmbhatt, S., Miezin, F.M., et al., 2007. Development of distinct control networks through segregation and integration. Proc. Natl. Acad. Sci. U. S. A. 104, 13507–13512.
Fair, D.A., Cohen, A.L., Power, J.D., Dosenbach, N.U., Church, J.A., Miezin, F.M., et al., 2009. Functional brain networks develop from a "local to distributed" organization. PLoS Comput. Biol. 5, e10001381.
Feinberg, I., Campbell, I.G., 2010. Sleep EEG changes during adolescence: an index of fundamental brain reorganization. Brain Cogn. 72, 56–65.
Fontanini, A., Katz, D.B., 2008. Behavioral states, network states and sensory response variability. J. Neurophysiol. 100, 1160–1168.
Ghemlin, D., Thomas, C., Weisbrod, M., Walther, S., Resch, F., Oelkers-Ax, K., 2011. Development of brain synchronisation within school-age—individual analysis of resting (alpha) coherence in a longitudinal data set. Clin. Neurophysiol. 122, 1973–1983.
Giedd, J.N., 2004. Structural magnetic resonance imaging of the adolescent brain. Ann. N. Y. Acad. Sci. 1021, 77–85.
Giedd, J.N., Blumenthal, J., Jeffries, N.O., Castellanos, F.X., Liu, H., Zijdenbos, A., Paus, T., Evans, A.C., Rapoport, J.L., 1999. Brain development during childhood and adolescence: a longitudinal MRI study. Nat. Neurosci. 2, 861–863.
Gogtay, N., Giedd, J.N., Lusk, L., Hayashi, K.M., Greenstein, D., Vaituzis, A.C., et al., 2004. Dynamic mapping of human cortical development during childhood through early adulthood. Proc. Natl. Acad. Sci. U. S. A. 101, 8174–8179.
Groppe, D.M., Urbach, T.P., Kutas, M., 2011. Mass univariate analysis of event-related brain potentials/fields I: a critical tutorial review. Psychophysiology 48, 1711–1725.
Hipp, J.F., Hawellek, D.J., Corbetta, M., Siegel, M., Engel, A.K., 2012. Large-scale cortical correlation structure of spontaneous oscillatory activity. Nat. Neurosci. 15, 884–890.
Horton, J.C., Adams, D.L., 2005. The cortical column: a structure without function. Philos. Trans. R. Soc. Lond. B Biol. Sci. 360, 837–862.
Horwitz, B., 2003. The elusive concept of brain connectivity. NeuroImage 19, 466–470.
Hughes, J.R., John, E.R., 1999. Conventional and quantitative electroencephalography in psychiatry. J. Neuropsychiatry Clin. Neurosci. 11, 190–208.
Kaiser, M., 2011. A tutorial in connectome analysis: topological and spatial features of brain networks. NeuroImage 57, 892–907.
Kenet, T., Bibitchkov, D., Tsodyks, M., Grinvald, A., Arieli, A., 2003. Spontaneously emerging cortical representations of visual attributes. Nature 425, 954–956.
Koening, T., Prichep, L., Lehmann, D., Sosa, P.V., Braeker, E., Kleinlogel, H., Isenhart, R., John, E.R., 2002. Millisecond by millisecond, year by year: normative EEG microstates and developmental stages. NeuroImage 16, 41–48.
Kurth, S., Ringli, M., Geiger, A., LeBourgeois, M., Jenni, O.G., Huber, R., 2010. Mapping of cortical activity in the first two decades of life: a high-density sleep electroencephalogram study. J. Neurosci. 30, 13211–13219.
Lauf, H., 2008. Endogenous brain oscillations and related networks detected by surface EEG-combined fMRI. Hum. Brain Mapp. 29, 762–769.
Lippé, S., Kovacevic, N., McIntosh, A.R., 2009. Differential maturation of brain signal complexity in the human auditory and visual system. Front. Hum. Neurosci. 3, 48.
Liu, Z., Fukunaga, M., de Zwart, J.A., Duyn, J.H., 2010. Large-scale spontaneous fluctuations and correlations in brain electrical activity observed with magnetoencephalography. NeuroImage 51, 102–111.
Llinás, R.R., Ribary, U., Jeanmonod, D., Kronberg, E., Mitra, P.P., 1999. Thalamocortical dysrhythmia: a neurological and neuropsychiatric syndrome characterized by magnetoencephalography. Proc. Natl. Acad. Sci. U. S. A. 96, 15222–15227.
Llinás, R., Urbano, F., Leznik, E., Ramizeriz, R., van Marle, H.J., 2005. Rhythmic and dysrhythmic thalamocortical dynamics: GABA systems and the edge effect. Trends Neurosci. 28, 325–333.
Logothetis, N.K., Murayama, Y., Augath, M., Steffen, T., Werner, J., Oeltermann, A., 2009. How not to study spontaneous activity. NeuroImage 45, 1080–1089.
Lüchinger, R., Michels, L., Martin, E., Brandeis, D., 2012. Brain state regulation during normal development: Intrinsic activity fluctuations in simultaneous EEG-fMRI. NeuroImage 60, 1426–1439.
MacLean, J.N., Watson, B.O., Aaron, G.B., Yuster, R., 2005. Internal dynamics determine the cortical response to thalamic stimulation. Neuron 48, 811–823.
Manly, B.F.J., 1997. Randomization, Bootstrap and Monte Carlo Methods in Biology. 2nd ed. Chapman & Hall.
Marshall, P.J., Bar-Haim, Y., Fox, N.A., 2002. Development of the EEG from 5 months to 4 years of age. Clin. Neurophysiol. 113, 1199–1208.
McIntosh, A.R., Kovacevic, N., Itier, R.J., 2008. Increased brain signal variability accompanies lower behavioral variability in development. PLoS Comput. Biol. 4, e1000106.
Michels, L., Muthuraman, M., Lüchinger, R., Martin, E., Anwar, A.R., Raethjen, J., et al., 2013. Developmental changes of functional and directed resting-state connectivities associated with neuronal oscillations in EEG. NeuroImage 81, 231–242.
Newman, M.E.J., 2004. Analysis of weighted networks. Phys. Rev. E 70, 056131.
Nolte, G., Bai, O., Wheaton, L., Mari, Z., Vorbach, S., Hallett, M., 2004. Identifying true brain interaction from EEG data using the imaginary part of coherency. Clin. Neurophysiol. 115, 2292–2307.
Northoff, G., Duncan, N.W., Hayes, D.J., 2010. The brain and its resting state activity—experimental and methodological implications. Prog. Neurobiol. 92, 593–600.
Nunez, P.L., Srinivasan, R., 2006. Electric Fields of the Brain: The Neurophysics of EEG. Oxford University Press.
Palva, S., Palva, J.M., 2012. Discovering oscillatory interaction networks with M/EEG: challenges and breakthroughs. Trends Cogn. Sci. 16, 219–230.
Paus, T., 2007. Maturation of structural and functional connectivity in the human brain. In: Jirsa, V.K., McIntosh, A.R. (Eds.), Handbook of brain connectivity. Springer-Verlag, Berlin, pp. 463–476.
Paus, T., Keshavan, M., Giedd, J.M., 2008. Why do many psychiatric disorders emerge during adolescence? Nat. Rev. Neurosci. 9, 947–957.
Poulsen, C., Picton, T.W., Paus, T., 2009. Age-related changes in transient and oscillatory brain responses to auditory stimulation during early adolescence. Dev. Sci. 12, 220–235.
R Development Core Team, 2008. R: a language and environment for statistical computing Retrieved from http://www.r-project.org.
Raichle, M.E., 2010. Two views of brain function. Trends Cogn. Sci. 14, 180–190.
Ringach, D.L., 2009. Spontaneous and driven cortical activity: implications for computation. Curr. Opin. Neurobiol. 19, 439–444.
Rodríguez-Martínez, E.I., Barriga-Paulino, C.I., Rojas-Benjumea, M.A., Gómez, C.M., 2015. Co-maturation of theta and low-beta rhythms during child development. Brain Topogr. 28, 250–260.
Rubinov, M., Sporns, O., 2010. Complex network measures of brain connectivity: uses and interpretations. NeuroImage 52, 1059–1069.
Schäfer, C.B., Morgan, B.R., Ye, A.X., Taylor, M.J., Doesburg, S.M., 2014. Oscillations, networks, and their development: MEG connectivity changes with age. Hum. Brain Mapp. 35, 5249–5261.
Schulman, J.J., Cancro, R., Lowe, S., Lu, F., Walton, K.D., Llinás, R.R., 2011. Imaging of thalamocortical dysrhythmia in neuropsychiatry. Front. Hum. Neurosci. 5, 69.
Segalowitz, S.J., Santesso, D.L., Jetha, M.K., 2010. Electrophysiological changes during adolescence: a review. Brain Cogn. 72, 86–100.
Shaw, P., Kabani, N.J., Lerch, J.P., Eckstrand, K., Lenroot, R., Gogtay, N., et al., 2008. Neurodevelopmental trajectories of the human cerebral cortex. J. Neurosci. 28, 3586–3594.
Singh, K.D., 2012. Which "neural activity" do you mean? fMRI, MEG, oscillations and neurotransmitters. NeuroImage 62, 1121–1130.
Smit, D.J., Boersma, M., Schanck, H.G., Micheloyannis, S., Boomsma, D.I., Hulshoff Pol, H.E., et al., 2012. The brain matures with stronger functional connectivity and decreased randomness of its network. PLoS One 7, e36896.
Somsen, R.J., van't Klooster, B.J., van der Molen, M.W., van Leeuwen, H.M., Licht, R., 1997. Growth spurts in brain maturation during middle childhood as indexed by EEG power spectra. Biol. Psychol. 44, 187–209.
Sporns, O., 2011. Networks of the Brain. The MIT Press, Cambridge, MA.
Sporns, O., Tononi, G., Edelman, G.M., 2000. Theoretical neuroanatomy: relating anatomical and functional connectivity in graphs and cortical connection matrices. Cereb. Cortex 10, 127–141.
Srinivasan, R., 1999. Spatial structure of the human alpha rhythm: global correlation in adults and local correlation in children. Clin. Neurophysiol. 110, 1351–1362.
Stam, C.J., van Straaten, E.C., 2012. The organization of physiological brain networks. Clin. Neurophysiol. 123, 1067–1087.
Stevens, M.C., 2009. The developmental cognitive neuroscience of functional connectivity. Brain Cogn. 70, 1–12.
Supekar, K., Musen, M., Menon, V., 2009. Development of large-scale functional brain networks in children. PLoS Biol. 7, e1000157.
Teipel, S.J., Pogarell, O., Meindl, T., Dietrich, O., Sydykova, D., Hunklinger, U., et al., 2009. Regional networks underlying interhemispheric connectivity: an EEG and DTI study in healthy ageing and amnestic mild cognitive impairment. Hum. Brain Mapp. 30, 2098–2119.
Thatcher, R.W., 1992. Cyclic cortical reorganization during early childhood. Brain Cogn. 20, 24–50.
Thatcher, R.W., Biver, C., McAlaster, R., Salazar, A., 1998. Biophysical linkage between MRI and EEG coherence in closed head injury. NeuroImage 8, 307–326.
Thatcher, R.W., North, D.M., Biver, C.J., 2008. Development of cortical connections as measured by EEG coherence and phase delays. Hum. Brain Mapp. 29, 1400–1415.

Uhlhaas, P., Roux, F., Singer, W., Haenschel, C., Sireteanu, R., Rodriguez, E., 2009. The development of neural synchrony reflects late maturation and restructuring of functional networks in humans. Proc. Natl. Acad. Sci. U. S. A. 106, 9866–9871.
Uhlhaas, P., Roux, F., Rodriguez, E., Rotarska-Jagiela, A., Singer, W., 2010. Neural synchrony and the development of cortical networks. Trends Cogn. Sci. 14, 72–80.
Vakorin, V.A., Lippé, S., McIntosh, A.R., 2011. Variability of brain signals processed locally transforms into higher connectivity with brain development. J. Neurosci. 31, 6405–6413.
Vakorin, V.A., McIntosh, A.R., Mišić, B., Krakovska, O., Poulsen, C., Martinu, K., Paus, T., 2013. Exploring age-related changes in dynamical non-stationarity in electroencephalographic signals during early adolescence. PLoS One 8, e57217.
Valdés-Hernández, P.A., Ojeda-González, A., Martínez-Montes, E., Lage-Castellanos, A., Virués-Alba, T., Valdés-Urrutia, L., Valdes-Sosa, P.A., 2010. White matter architecture rather than cortical surface area correlates with the EEG alpha rhythm. NeuroImage 49, 2328–2339.
van den Heuvel, M.P., Stam, C.J., Kahn, R.S., Hulshoff Pol, H.E., 2009. Efficiency of functional brain networks and intellectual performance. J. Neurosci. 29, 7619–7624.
van Diessen, E., Numan, T., van Dellen, E., van der Kooi, A.W., Boersma, M., Hofman, D., et al., 2014. Opportunities and methodological challenges in EEG and MEG resting state functional brain network research. Clin. Neurophysiol. (in press).
Varela, F., Lachaux, J.P., Rodriguez, E., Martinerie, J., 2001. The brainweb: phase synchronization and large-scale integration. Nat. Rev. Neurosci. 2, 229–239.
Vértes, P.E., Bullmore, E.T., 2015. Annual research review: growth connectomics—the organization and reorganization of brain networks during normal and abnormal development. J. Child Psychol. Psychiatry 56, 299–320.
Whitford, T.J., Rennie, C.J., Grieve, S.M., Clark, C.R., Gordon, E., Williams, L.M., 2007. Brain maturation in adolescence: concurrent changes in neuroanatomy and neurophysiology. Hum. Brain Mapp. 28, 228–237.